

# Protracted Developmental Trajectory of Shape Processing along the Two Visual Pathways

Erez Freud<sup>1,2</sup>, David C. Plaut<sup>2</sup>, and Marlene Behrmann<sup>2</sup>

## Abstract

■ Studies of the emergence of shape representations in childhood have focused primarily on the ventral visual pathway. Importantly, however, there is increasing evidence that, in adults, the dorsal pathway also represents shape-based information. These dorsal representations follow a gradient with more posterior regions being more shape-sensitive than anterior regions and with representational similarity in some posterior regions that is equivalent to that observed in some ventral regions. To explore the emergence and nature of dorsal shape representations in development, we acquired both fMRI BOLD signals and behavioral data in children (aged 8–10 years) using a

parametric image scrambling paradigm. Children exhibited adult-like large-scale organization of shape processing along both ventral and dorsal pathways. Also, as in adults, the activation profiles of children's posterior dorsal and ventral regions were correlated with recognition performance, reflecting a possible contribution of these signals to perception. There were age-related changes, however, with children being more affected by the distortion of shape information than adults, both behaviorally and neurally. These findings reveal that shape-processing mechanisms along both dorsal and ventral pathways are subject to a protracted developmental trajectory. ■

## INTRODUCTION

Shape representations in the human visual cortex are essential for fundamental visual abilities, such as object recognition, face perception, and reading. Following the well-known two cortical visual systems hypothesis (Goodale & Milner, 1992; Ungerleider & Mishkin, 1982), the majority of research on the development of sensitivity to the geometry of visual shapes has focused on the ventral “what” visual pathway (Saygin et al., 2016; Scherf, Thomas, Doyle, & Behrmann, 2014; Kravitz, Saleem, Baker, Ungerleider, & Mishkin, 2013; Golarai et al., 2007; Scherf, Behrmann, Humphreys, & Luna, 2007; e.g., Emberson, Crosswhite, Richards, & Aslin, 2017; Gomez et al., 2017). A key finding from these studies is that there are different developmental trajectories for different visual categories in ventral cortex, with selectivity for objects and places observed relatively early, followed later by the emergence of selectivity for faces and words (Liu et al., 2018; Gomez et al., 2017; Scherf et al., 2007, 2014; Golarai et al., 2007).

Despite the early emergence of object-selective cortical regions (Emberson et al., 2017) and the stability in the size of these regions across development (Golarai et al., 2007), neural representations derived by these regions are still modulated as a function of age. For example, Nishimura, Scherf, Zachariou, Tarr, and Behrmann (2015) noted that lateral occipital cortex (LOC) representations in children

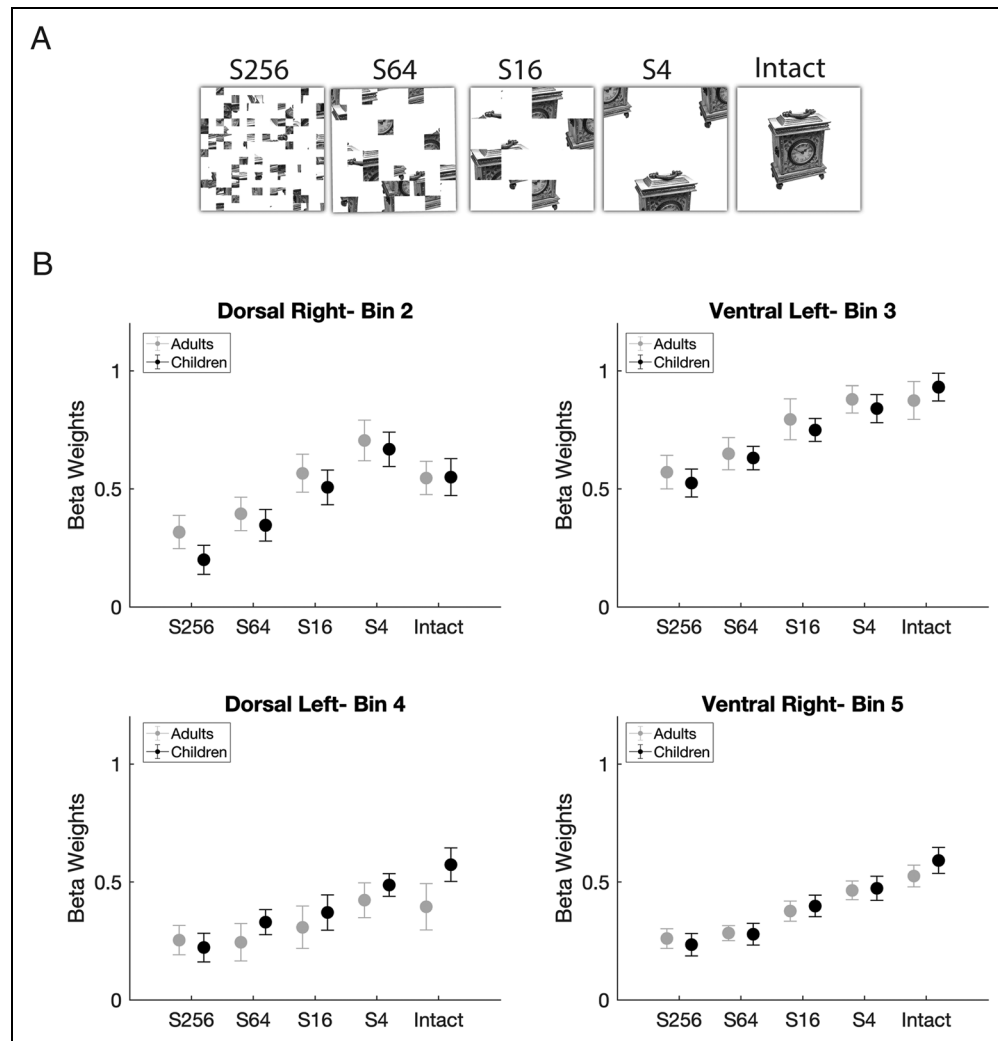
aged 5–10 years were invariant to object size, but not to object viewpoint. In contrast, the mature LOC exhibits invariant response profiles to both of these stimulus dimensions (Grill-Spector & Malach, 2004).

Interestingly, recent evidence from investigations with adults and with nonhuman primates suggests that the dorsal (“where/how”) pathway also derives shape representations and that these representations play a functional role in perception (e.g., Freud, Robinson, & Behrmann, 2018; Freud, Ganel, et al., 2017; Van Dromme, Premereur, Verhoef, Vanduffel, & Janssen, 2016; Vaziri-Pashkam & Xu, 2017; Bracci & Op de Beeck, 2016; Konen & Kastner, 2008; for a review, see Freud, Plaut, & Behrmann, 2016). To date, however, only a few studies have investigated the developmental trajectory of shape perception in the dorsal visual pathway. These studies have focused primarily on visuo-motor representations and, using pictures of tools, have documented adult-like organization of the tool network in children aged 6–10 years (Kersey, Clark, Lussier, Mahon, & Cantlon, 2015; Dekker, Mareschal, Sereno, & Johnson, 2011). Importantly, those studies focused on high-level category-selective activation and did not explore to what extent shape information is represented by both pathways. Moreover, given the strong visuomotor association afforded by tools, it is unclear whether these dorsal responses reflect computations related to the visuomotor or perceptual information conveyed by these stimuli and whether there are possible age-based effects in this pathway.

To describe the large-scale organization of shape processing in children, we utilized an approach that has

<sup>1</sup>York University, Toronto, <sup>2</sup>Carnegie Mellon University

**Figure 1.** (A) Experimental stimuli and (B) raw beta weights. (A) Box scrambling manipulation. Shape information was altered by dividing the display using an invisible grid and then randomly rearranging the squares. (B) Beta weights in four representative bins, two of which are derived from the dorsal and two from the ventral pathways. In all bins, the linear fit ( $R^2$ ) was found to be greater than .3, and the linear fit was similar across the two groups.



been successful in mapping shape representations in adults (Freud, Culham, Plaut, & Behrmann, 2017). This approach entails presenting participants with images of a wide range of objects, parametrically scrambled across five levels, while acquiring BOLD data in an fMRI scanner. The slope of the decrease in the BOLD signal across levels of scrambling then provides a fine-grained characterization of relative sensitivity to shape information in each voxel in both ventral and dorsal pathways (see Figure 1B and Methods). Recognition of these same displays was measured outside the magnet, and brain-behavior correlations were analyzed. Last, both neural and psychological comparisons to the adult profile were undertaken.

## METHODS

### Participants

Eleven right-handed children (mean age = 9.17 years, range = 8–10.25 years, five girls) completed the experiment. The data from Experiment 1 of Freud, Culham, et al. (2017) provided the comparison adult profile (11 participants, mean age = 31 years, range = 19–46 years, two women). However, as children completed only four experimental runs, we used as

our comparison data the first four runs (out of eight) of the data from the adult experiment. All participants were compensated for their participation and provided assent, and their parents provided informed consent for them to participate in the protocol, which was approved by the institutional review board of Carnegie Mellon University.

### Stimuli

Stimuli were 80 grayscale pictures of everyday objects (40 pictures) and tools (40 pictures) identical to those presented in a previous publication (Freud, Culham, et al., 2017) but excluding four pictures of objects that children were unlikely to recognize (e.g., VCR cassette). We employed an algorithm that divided and randomly rearranged each image into 4, 16, 64 and 256 squares, resulting in five levels of scrambling (Figure 1A).

### Experimental Design

#### fMRI

Participants viewed the stimuli (visual angle of  $4.5^\circ \times 4.5^\circ$ ) in a pseudorandomized order through a mirror

setup that reflected a liquid crystal display screen located at the back of the scanner bore. Before entering the magnet, participants completed a short training session in a mock scanner to acclimate them to the MRI environment and noise and to minimize head movements.

### *MRI Setup*

Participants were scanned in a Siemens Verio 3-Tesla magnetic resonance imaging scanner with a 32-channel coil at Carnegie Mellon University. We acquired a structural scan using a T1-weighted protocol that included 176 sagittal slices (1 mm thickness, in-plane resolution = 1 mm, matrix =  $256 \times 256$ , repetition time = 2300 msec, echo time = 1.97 msec, inversion time = 900 msec, flip angle =  $9^\circ$ ). We employed a gradient-echo, echoplanar imaging sequence (repetition time = 1.5 sec, echo time = 30 msec, flip angle =  $73^\circ$ ) to acquire the functional images based on the BOLD signal. Each run (total of four) included 227 volumes of 43 axial slices (slice thickness = 3 mm, gap = 0 mm, in-plane resolution = 3 mm).

### *Object Scrambling Experiment*

In each of the four runs, participants viewed pictures that were blocked by the five levels of scrambling (S256, S64, S16, S4, and Full [intact]) and by category (tools and objects). After an initial fixation of 10.5 sec, the experiment included twenty 9-sec blocks, each composed of 10 stimuli with each image displayed for 600 msec followed by 300 msec fixation. The blocks were separated by 7.5-sec fixation periods. Participants fixated on the cross in the center of the display and performed a task that was orthogonal to the presentation of the objects. Specifically, throughout the scan, participants indicated, via a button press, when the color of the fixation cross changed from black to red. There were one or two fixation color changes per block of 10 stimuli.

### *Object Recognition (Behavioral) Experiment*

Children (10 of 11) and adults (11 of 11) completed the object recognition experiment after the fMRI scan (range: same day to 30 days). The participants were seated 50 cm in front of a computer screen in a darkened room, shown the same stimuli they had viewed in the scanner and instructed to name aloud each stimulus. The experimenter tracked the accuracy of their recognition responses. Stimuli were presented in a pseudorandomized fashion, for 600 msec (as in the fMRI experiment), with each picture presented once.

## **Statistical Analyses**

### *Univariate Analysis*

The raw fMRI data of children are available at DOI: 10.1184/R1/c.4122161, and the adult data were taken from DOI:

10.1184/R1/c.3889873.v1. We analyzed the data using BrainVoyager 20.2 software (Brain Innovation, Maastricht, The Netherlands), in-house scripts written in MATLAB (The MathWorks, Inc.) and JASP (JASP Team, 2018). Preprocessing included 3-D motion correction and filtering of low temporal frequencies (cutoff frequency of 2 cycles per run). We did not apply spatial smoothing to allow the voxel-wise analysis. We transformed all scans to Montreal Neurological Institute (MNI) space.

The first step of the analytic approach was based on the voxel-wise analysis employed in the previous study with adult participants (Freud, Culham, et al., 2017). We generated a group-level mask of all visually selective voxels by performing a random-effects general linear model analysis across all 22 participants (children and adults). For each voxel, we tested whether it was reliably responsive to any of the five conditions relative to fixation (scrambling level: S256, S64, S16, S4, Intact;  $t > 2.6$ ). We included all visually sensitive voxels in the mask, which was then applied in the individual subject analysis.

Next, we calculated the slope of activation (beta values) as a function of scrambling level separately for each participant in each visually selective voxel. A positive slope reflects an increase in activation as the level of scrambling decreases (from S256 to Intact) and therefore reflects greater shape sensitivity. A negative slope represents a decrease in activation as the level of scrambling decreases and, as such, may reflect greater sensitivity to local elements and edges, which are more frequent in increasingly distorted images.

### *Head Motion*

We calculated head motion from each run and from each participant using a combination of three translation parameters (in millimeters) and three rotation parameters (in degrees):

$$\text{Total translation} = \sqrt{d(x)^2 + d(y)^2 + d(z)^2}$$

$$\text{Total rotation} = \sqrt{r(x)^2 + r(y)^2 + r(z)^2}$$

Larger head movements were noted for the children than the adults for rotation (children:  $0.5 \pm 0.21$  degree; adults:  $0.21 \pm 0.14$  degree),  $t(20) = -2.402$ ,  $p = .026$ , Cohen's  $d = -1.024$ , and translation (children:  $0.63 \pm 0.30$  mm; adults:  $0.26 \pm 0.11$  mm),  $t(20) = 3.789$ ,  $p = .001$ , Cohen's  $d = -1.616$ . We discuss these differences in the results section and consider their impact on the neural data.

### *Temporal Signal-to-Noise Ratio*

We calculated the temporal signal-to-noise ratio (tSNR) to compare fMRI data quality across participants. For each

run, tSNR was calculated as the mean signal of the fMRI time series divided by the standard deviation of the noise in the time series:  $\text{SNR}(\text{temporal}) = \mu \text{ time series} / \sigma \text{ time series}$ . Consistent with the head motion analysis, we found reduced tSNR for the children ( $132.5 \pm 12.8$ ) than for the adults ( $146.5 \pm 11.8$ ),  $t(20) = 2.645$ ,  $p = .016$ , Cohen's  $d = 1.128$ . The results were replicated when only visual-selective voxels were included in the analysis. We interpret this difference in the context of the experimental results in the Results section.

### *Intersubject Functional Correlation*

To estimate the similarity between the large-scale organization of shape processing across the two groups, we utilized the intersubject functional correlation (ISFC; Rosenthal et al., 2017; Simony et al., 2016). ISFC is designed to uncover the stimulus-locked functional responses by correlating the response profiles across participants. First, for each group (children/adults), we correlated voxel-wise shape sensitivity values (i.e., slopes) between each participant and the mean voxel shape sensitivity calculated over all the remaining participants (within-group similarity). Next, using the same procedure, we calculated the correlation between each participant and the mean voxel shape sensitivity calculated over all the participants from the other group (between-groups similarity). Finally, we transformed (Fisher  $Z$ ) the correlation coefficients and compared the within-/between-groups correlations.

### *Bin Analysis*

To compare between shape sensitivity across the two groups in a more direct fashion, for each individual, we divided each pathway into five bins based on the voxel's  $y$ -axis coordinate (posterior–anterior). Next, for each bin, we calculated the average shape sensitivity (slope). We obtained similar results when we divided the bins based on the distance from the most posterior voxel, as calculated by a combination of the  $x$  (lateral–medial) and  $y$  (posterior–anterior) axes.<sup>1</sup> To calculate the interaction between bin and other factors, we applied the Huyhn–Feldt sphericity correction, because sphericity assumption was violated (Mauchly's  $W$ ;  $p < .05$ ). Note that all the reported results hold even when the correction was not applied.

### *Correlation with Object Recognition*

To examine the correlation between fMRI activation and behavioral performance, we used the bins as ROIs. Notably, we observed similar results when we defined regions based on a probabilistic atlas (Wang, Mruczek, Arcaro, & Kastner, 2015).

The univariate analyses described above included just five levels of scrambling, limiting the ability to calculate a

reliable correlation between participants' BOLD response and object recognition ability. We therefore divided the fMRI data into two data sets (odd and even runs), in which different objects were presented, and we separated the data into BOLD obtained from the tools and object categories. This procedure yielded 20 beta weights for each ROI. We split the behavioral data into 20 subsets, as was done with the neural data, and computed the partial correlations between behavioral performance and fMRI signal, controlling for the correlation of these two variables with the level of scrambling. Note that similar results were obtained when only 5 data points were extracted from each bin and when full (rather than partial) correlations were calculated.<sup>1</sup>

## **RESULTS**

The presentation of the results is organized into four sections: First, we validate that a linear function of fMRI activation describes shape sensitivity in both groups. Next, we compare the large-scale organization of shape processing along the dorsal and ventral visual pathways in children versus adults based on the ISFC and the bin analysis approaches. Thereafter, for both groups, we present the behavioral recognition accuracy as a function of scrambling level, and finally, we report the correlation between the neural and behavioral profiles. Together, these analyses provide a full characterization of object sensitivity in dorsal and ventral pathways in the children, and the measures derived from the children can be compared directly to the adult object sensitivity profile.

### **fMRI Results**

#### *Linear Function Describes Shape Sensitivity in Both Groups*

First, we sought to establish that shape sensitivity could be reliably described by the linear slope between the beta weights, as was done previously in adults. This step was particularly important given the observed differences in tSNR between the two groups (see Methods for details). To this end, each pathway was divided into five bins, and the beta-weights for each condition (image type) was calculated. Next, the linear slope was calculated for each of the bins, separately for each participant, and we compared between the two groups.

For illustration purposes, Figure 1B depicts the raw beta values, for the two groups, in several representative bins. In both groups, in all bins, the linear fit ( $R^2$ ), ranging from .3 to .84, was reliably above zero ( $p < .05$ , FDR-corrected, excluding one bin in the children's group in which  $p\text{FDR} = .06$ ). Next, a series of  $t$  tests confirmed that the linear fit was not different between the groups across all bins ( $p > .39$ , FDR-corrected). Finally, we also validated that the raw response for the intact objects (i.e., the baseline condition) was similar between the groups across all bins ( $p > .39$ ,

FDR-corrected). Together, these findings suggest that, despite the reduced tSNR in the children group, the linear slope can still be utilized as an indicator of shape sensitivity in both adults and children.

### Preserved Large-Scale Organization of Shape Processing

At the outset, a voxel-wise map of shape sensitivity was generated separately for every participant. Similar to our previous study (Freud, Culham, et al., 2017), in each voxel, beta weights were extracted for each of the five stimulus conditions from most scrambled to intact (S256, S64, S16, S4, Full), and the linear slope between these conditions was used as an index of shape sensitivity (i.e., greater positive slopes reflect greater shape sensitivity). Next, we used the ISFC approach (Rosenthal et al., 2017; Simony et al., 2016) to compare the large-scale organization of shape processing across the two groups.

Although we used only half of the data originally acquired for each adult participant in Freud, Culham, et al. (2017; to equate the amount of data for adults and children), the findings from the adult group replicated the large-scale organization of shape sensitivity along both the ventral and dorsal pathways observed with the full data set. In both pathways, negative slopes were found in posterior occipital cortex (greater sensitivity to maximal scrambling condition), whereas positive slopes (greater sensitivity to more intact images) emerged in more anterior parts (i.e., dorsal pathway: posterior intraparietal sulcus, ventral pathway: inferior surface of the occipitotemporal cortex). In even more anterior regions (i.e., dorsal pathway: anterior intraparietal sulcus, ventral pathway: anterior and medial temporal cortex), a decrease in shape sensitivity was detected (Figure 2A). Importantly, a similar, large-scale organization was obtained for the children's data (Figure 2B).

To estimate statistically the similarity of the topographical organization of shape-selective voxels between the two groups, we generated within- and between-groups similarity indices using the ISFC approach. This method calculates the voxel-wise correlations of the brains of different participants who belong to the same group or to different groups (see Methods for details).

First, we sought to establish that shape selectivity varied with the spatial location of the voxels in a similar fashion across the two groups. Interestingly, in both dorsal and ventral pathways, we found reliable between-groups similarity (i.e., correlations greater than zero),  $t(21) > 12.04$ ,  $p < .000000002$ , Cohen's  $d > 2.567$  (Figure 2D).

Next, we employed a repeated-measures ANOVA with ISFC type (within group, between groups), Pathway (dorsal, ventral), and Hemisphere (right, left) as independent variables. This analysis revealed that the within-group correlations (mean = .7) were slightly but significantly greater than the between-groups correlation (mean = .67),  $F(1, 20) = 4.637$ ,  $p = .043$ ,  $\eta_p^2 = .18$ . This latter effect provides the first evidence that, despite the qualitative similarity between the large-scale organization of shape

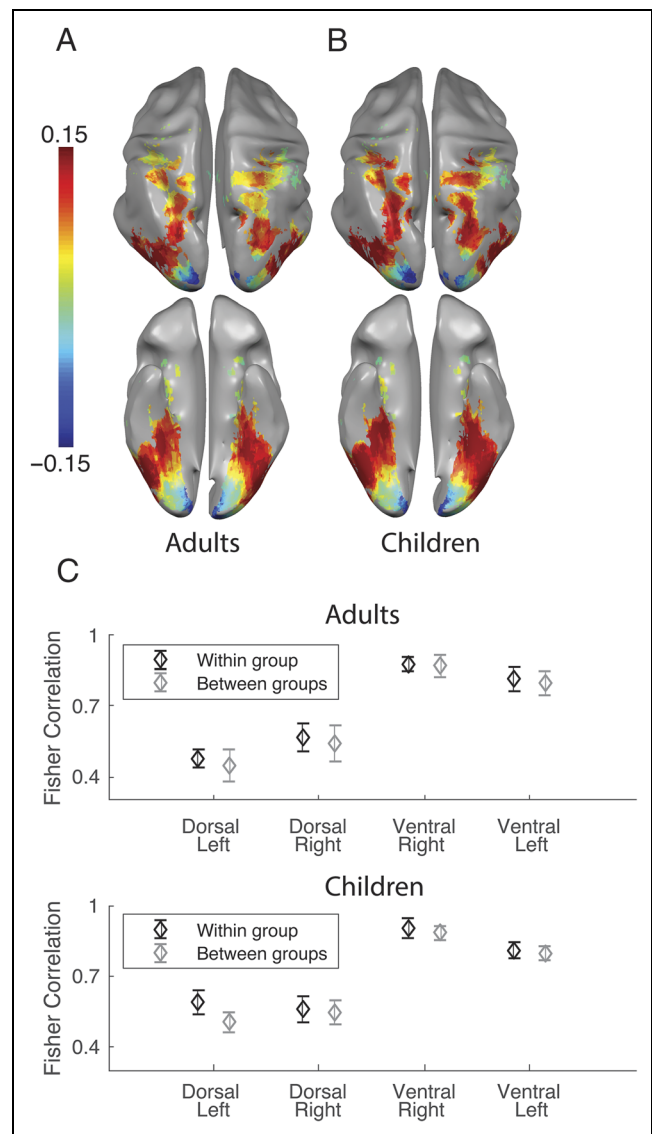


**Figure 2.** (A–C) fMRI results. The (A) adults and (B) children groups are projected on an inflated brain from a superior view (upper panel) and from a posterior–inferior view (lower panel). Warm colors signify voxels that are shape-sensitive (positive slopes), with activation increasing as a function of object coherence. Conversely, cold colors reflect low shape sensitivity (negative slopes) or greater sensitivity for scrambled than intact images. (C) Intersubject correlation analysis revealed significant between-groups correlations in both dorsal and ventral pathways of both hemispheres reflecting the similarity in the large-scale organization of shape processing along the two groups. However, within-group correlations were greater, uncovering some differences between the two groups.

processing across the two groups, shape sensitivity changes over development.

We also found a robust effect for Pathway,  $F(1, 20) = 75$ ,  $p < .001$ ,  $\eta_p^2 = .79$ , with greater similarity within the ventral pathway than within the dorsal pathway. This difference might indicate that more reliable shape representations are derived by the ventral pathway. Finally, there was no main effect of Group, nor an interaction of Group with any of the other factors ( $F_s < 1$ ).

Note that, to the extent that there were any differences between the two groups, factors other than age may be implicated. First, as reported above, children moved more than adults in the magnet and had a lower tSNR. Second, spatial normalization to MNI space might differently affect the two groups, because the MNI atlas is based on the mature brain. Therefore, in the next section, we analyze the differences between children and adults in greater detail to explore the underlying source of the group differences.

### Increased Sensitivity to Object Distortion in Childhood

To elucidate the differences between the two age groups, we divided each pathway into five bins along the posterior–anterior axis of the brain and directly compared shape sensitivity between the two groups using ANOVA. Figure 3 compares the two groups based on Pathway, Hemisphere, and Location along the  $y$  axis (divided into five bins). Interestingly, greater shape sensitivity was found for children in shape-selective bins in both the ventral and dorsal pathways. A repeated-measures ANOVA revealed that, despite a trend, the main effect for Group was not significant,  $F(1, 20) = 3.78, p = .06$ , and was qualified by a significant two-way interaction between Group and bins,  $F(1.549, 30.978) = 3.829, p < .05, \eta_p^2 = .16$ . Planned comparisons revealed greater slopes for children compared with adults in Bins 2–4 ( $F_s > 4.47, p \leq .05$ ; planned comparisons and an FDR correction yielded  $p$  values equal to .07 for each of these bins),

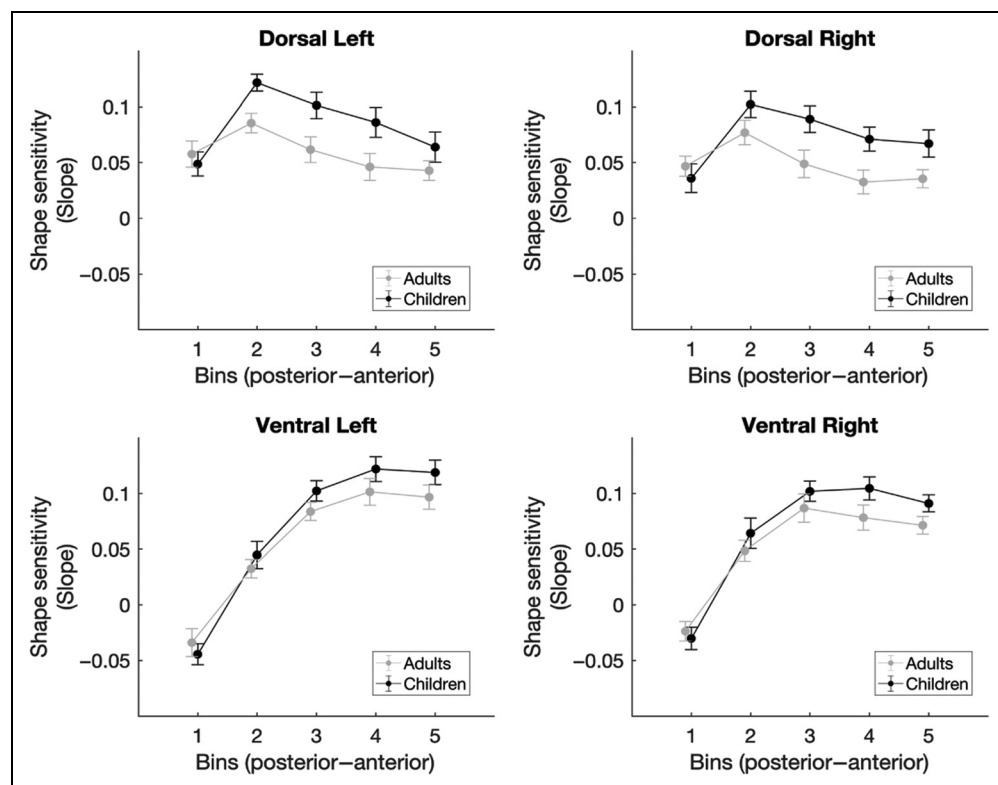
which map onto high-level object-selective regions along the two pathways.

Finally, we also identified a trend for an interaction between group and pathway, such that the differences between groups were more evident along the dorsal than the ventral pathway,  $F(1, 20) = 2.934, p = .102, \eta_p^2 = .128$ . The idea that the developmental trajectories of the two pathways are different has already been suggested in the past (Ciesielski et al., 2019); however, we did not elaborate further on this issue, given that the interaction is not significant.

The bin analysis provides novel evidence for the immaturity of object-selective regions not only in the ventral pathway but also along the dorsal pathway. In particular, children exhibit similar topographical organization of shape-selective regions as adults, but nevertheless, compared with the mature brain, these regions are more sensitive to the distortion of object information (as reflected by steeper slopes). Finally, to ensure that the observed results were not the product of the specific use of five bins, the bin analysis was repeated with different numbers of bins (8 and 10),<sup>1</sup> and the results reported above were replicated.

Importantly, the reported differences in tSNR and head motion between the two groups (see above) are unlikely to account for the differential between-groups shape sensitivity. In particular, given the increased motion and lower tSNR observed for the children over adult group, one might expect that these artifacts might result in lower beta values and/or lower shape sensitivity in this

**Figure 3.** Shape sensitivity along the two pathways. The average shape sensitivity as a function of group and bin: posterior (1) to anterior (5). In bins that included high-level shape-selective voxels (2–4), greater shape sensitivity (i.e., decrease in beta weights as a function of level of scrambling) was observed for the children group compared with the adults group.



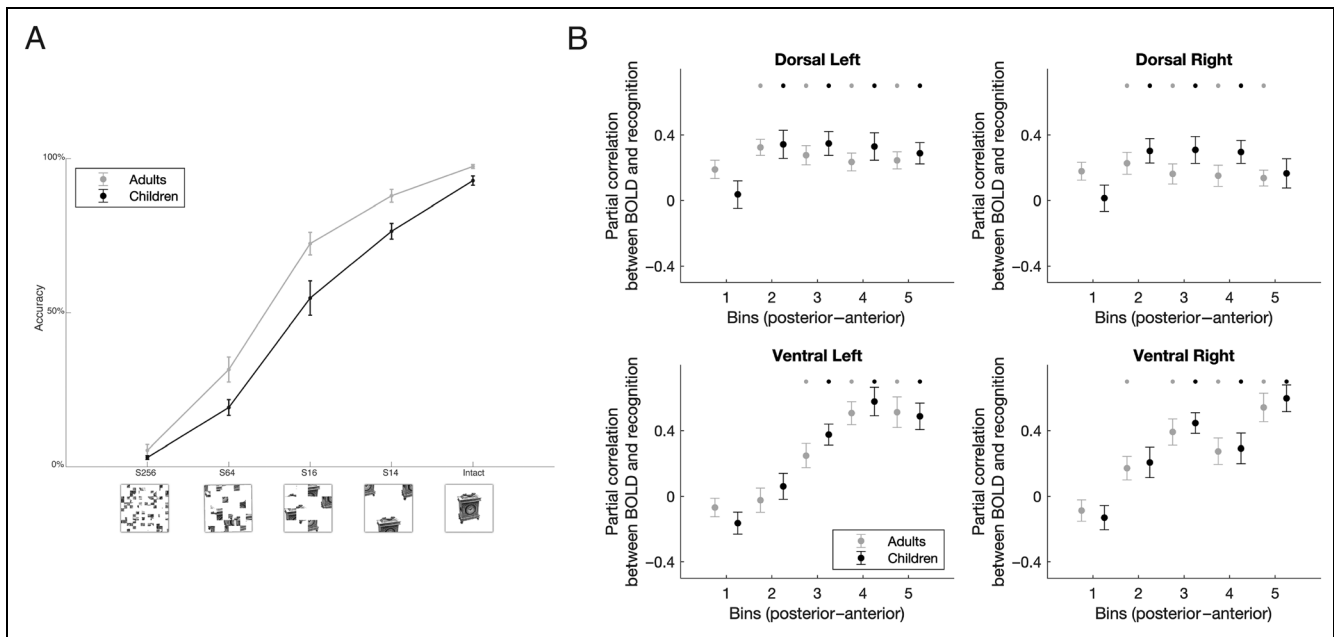


**Figure 4.** Correspondence between fMRI and object recognition performance. (A) Mean accuracy of recognition, obtained outside the scanner as a function of scrambling and group. Recognition ability decreased as a function of scrambling, but the effect of scrambling was more robust in the children group. (B) Partial correlation between fMRI activation and recognition performance along the two pathways. Black and gray asterisks signify that an ROI evidences a significantly positive correlation between these two variables ( $r > 0$ ,  $q < 0.05$ ) for the children and adult groups, respectively. In both groups, object recognition abilities were correlated with fMRI responses across different ROIs in the mid-anterior parts of the ventral pathway and mid-posterior parts of the dorsal pathways.

group. However, as demonstrated in multiple analyses (e.g., Figures 1B and 3), children had at least equivalent beta-weights compared with adults and greater shape sensitivity. Together, these findings suggest that, despite the differences in SNR, our experimental paradigm was still sufficiently sensitive to permit exploration of group differences.

### Behavioral Results

An important question raised by the fMRI results is whether the greater fMRI sensitivity to distortion in shape information among children would also be observed behaviorally. To address this question, after their fMRI scan (range: same day to 30 days), children and adults were shown the stimuli and asked to identify the object in the image by verbal response (Freud, Culham, et al., 2017).

A repeated-measures ANOVA with Group and Level of scrambling as independent variables and accuracy as the dependent variable revealed two main effects for the Level of scrambling,  $F(4, 76) = 730$ ,  $p < .0001$ ,  $\eta_p^2 = .975$ , and group,  $F(1, 19) = 8.963$ ,  $p = .007$ ,  $\eta_p^2 = .32$ . These effects were qualified by an interaction between these factors,  $F(4, 76) = 4.803$ ,  $p = .0016$ ,  $\eta_p^2 = .2$ . Planned comparisons revealed that adults were more accurate than children even for intact objects,  $F(1, 19) = 8.61$ ,  $p = .016$ , planned comparisons, FDR-corrected (Figure 4A). However, the adverse effect of scrambling was disproportionate in children, as the gap between the adults' and children's accuracy was greater for the

middle three scrambling levels than for the intact objects,  $F(1, 19) = 5.92$ ,  $p = .025$ , planned comparisons, FDR-corrected (the last scrambling level, S256, was excluded because performance was extremely low at ~4% and likely at floor in both groups). This result indicates that the children's enhanced neural sensitivity to object distortion was also evident in their perceptual behavior.

Finally, we calculated the partial correlation between the fMRI signal and the behavioral performance of each participant after regressing out the shared correlation with the level of scrambling. Similar to adults, fMRI activation in the children's group, along the anterior portions of the ventral pathway, was correlated with behavior, and the same was true for fMRI activation in the posterior dorsal pathway ( $r > 0$ ,  $p < .05$ , FDR-corrected; Figure 4B). No differences between the correlations of the two groups were observed (all  $ps > .3$ ).

### DISCUSSION

The developmental trajectory of shape representations in the visual cortex has been described largely in relation to the ventral visual cortex, with rather little attention to possible shape representations in the dorsal cortex. To uncover the large-scale organization of shape processing along both visual pathways during childhood, we derived a detailed description of shape sensitivity using a parametric scrambling manipulation (Freud, Culham, et al., 2017). We then compared the neural and behavioral profile of children versus adults, taking into account

the topographical organization of shape processing, the extent of the shape sensitivity, and the correspondence with object recognition performance.

Children and adults exhibited similar large-scale organization of shape processing along both visual pathways, with an initial increase followed by a subsequent decrease in shape sensitivity moving along the posterior-to-anterior axis. Although the spatial distribution of shape-selective voxels was correlated across the two groups, there were several quantitative differences. In particular, within-group correlations were greater than between-groups correlations, pointing to differences in the shape sensitivity profile along the two pathways for children versus adults. Accordingly, the analysis of the activation profile (computed across bins of voxels) revealed that, in children compared with adults, the slope of shape selectivity was steeper in high-level visual cortices, reflecting a greater increase in fMRI activity as more shape information was available. This latter finding was mirrored in object recognition performance in that, relative to adults, children's accuracy was poorer but, additionally, was disproportionately reduced as the level of scrambling increased. Thus, by the age of 8–10 years old, shape-processing mechanisms are already in place at a broad level, but are not fully mature.

These findings echo previous observations of the development of ventral pathway representations. In particular, in adulthood, LOC representations are known to be invariant to object size and viewpoint (Kourtzi, Erb, Grodd, & Bulthoff, 2003; Andresen, Vinberg, & Grill-Spector, 2009), but in young children roughly the same age as those tested in the current study, fMRI adaptation was observed to object size, but not to object viewpoint (Nishimura et al., 2015). Such findings confirm that there is early sensitivity of this region to object shape (Emberson et al., 2017), but that the underlying neural representations are still subject to a protracted developmental trajectory. This conclusion is also consistent with behavioral observations that have documented reduced sensitivity to object structural information and spatial organization in children (Freud, Culham, Namdar, & Behrmann, 2019; Freud & Behrmann, 2017; Kovács, Kozma, Fehér, & Benedek, 1999).

The key focus of the current study concerned the maturational profile of the dorsal visual pathway. Accumulating evidence suggests that the dorsal visual pathway, which is known to subserve visuomotor control, also derives shape representations that are independent of visuomotor properties (Vaziri-Pashkam & Xu, 2017; Bracci & Op de Beeck, 2016; Freud et al., 2016; Konen & Kastner, 2008). Moreover, these dorsal representations have been shown to be correlated with object recognition performance, suggesting that they may play a functional role in perception (Freud et al., 2018; Zachariou, Nikas, Safiullah, Gotts, & Ungerleider, 2017; Van Dromme et al., 2016).

To date, the developmental trajectory of shape representations in the dorsal pathway has been largely

unexplored: Previous studies have documented adult-like responses in the dorsal pathway, but the responses were obtained in experiments that included a visuomotor task (James & Kersey, 2017) or pictures of tools (Kersey et al., 2015; Dekker et al., 2011) that convey clear visuomotor associations. Here, we provide novel evidence that, similar to the ventral pathway, dorsal shape-processing mechanisms are present in childhood (8–10 years old), although they are not yet fully adult-like.

To conclude, this study provides novel insights into the development of shape-processing mechanisms along the two visual pathways, with careful scrutiny of the dorsal visual pathway, which has been somewhat neglected to date. Our findings point to two main conclusions. First, the role of the dorsal pathway in shape processing emerges relatively early in life. Second, despite the presence of a roughly adult-like mechanism of shape processing, the visual system is not fully adult-like and requires further tuning or refinement of its computations. Based on the existing findings, it is impossible to determine the precise time course of development in the two pathways, and future research with children younger than those who participated in this study should address this important question.

## Acknowledgments

The research reported here was supported by funding from Spatiotemporal Codes Underlying Face Recognition (PI: Plaut) PA Formula Award 2014, SAP 4100068709, and by a grant from the National Institutes of Health to M. B. (RO1 EY027018). E. F. was supported by the Vision Science to Applications (VISTA) program funded by the Canada First Research Excellence Fund (CFREF, 2016–2023). E. F. acknowledges the support of the Natural Sciences and Engineering Research Council of Canada (NSERC).

Reprint requests should be sent to Erez Freud, York University, 4700 Keele Street, Toronto, Ontario, Canada, M3J 1P3, or via e-mail: efreud@yorku.ca.

## Note

1. Note that the statistics of the complementary analyses described throughout the paper are available for download at: [http://freud.lab.yorku.ca/files/2019/05/complementary\\_analyses.pdf](http://freud.lab.yorku.ca/files/2019/05/complementary_analyses.pdf).

## REFERENCES

- Andresen, D. R., Vinberg, J., & Grill-Spector, K. (2009). The representation of object viewpoint in human visual cortex. *Neuroimage*, *45*, 522–536.
- Bracci, S., & Op de Beeck, H. (2016). Dissociations and associations between shape and category representations in the two visual pathways. *Journal of Neuroscience*, *36*, 432–444.
- Ciesielski, K. T. R., Stern, M. E., Diamond, A., Khan, S., Busa, E. A., Goldsmith, T. E., et al. (2019). Maturational changes in human dorsal and ventral visual networks. *Cerebral Cortex*. doi:10.1093/cercor/bhz053/5423756.

- Dekker, T., Mareschal, D., Sereno, M. I., & Johnson, M. H. (2011). Dorsal and ventral stream activation and object recognition performance in school-age children. *Neuroimage*, *57*, 659–670.
- Emberson, L. L., Crosswhite, S. L., Richards, J. E., & Aslin, R. N. (2017). The lateral occipital cortex (LOC) is selective for object shape, not texture/color, at 6 months. *Journal of Neuroscience*, *33*, 3300–3316.
- Freud, E., & Behrmann, M. (2017). The life-span trajectory of visual perception of 3D objects. *Scientific Reports*, *7*, 11034.
- Freud, E., Culham, J. C., Namdar, G., & Behrmann, M. (2019). Object complexity modulates the association between action and perception in childhood. *Journal of Experimental Child Psychology*, *179*, 56–72.
- Freud, E., Culham, J. C., Plaut, D. C., & Behrmann, M. (2017). The large-scale organization of shape processing in the ventral and dorsal pathways. *eLife*, *6*, e27576.
- Freud, E., Ganel, T., Shelef, I., Hammer, M. D., Avidan, G., & Behrmann, M. (2017). Three-dimensional representations of objects in dorsal cortex are dissociable from those in ventral cortex. *Cerebral Cortex*, *27*, 422–434.
- Freud, E., Plaut, D. C., & Behrmann, M. (2016). ‘What’ is happening in the dorsal visual pathway. *Trends in Cognitive Sciences*, *20*, 773–784.
- Freud, E., Robinson, A. K., & Behrmann, M. (2018). More than action: The dorsal pathway contributes to the perception of 3-D structure. *Journal of Cognitive Neuroscience*, *30*, 1047–1058.
- Golarai, G., Ghahremani, D. G., Whitfield-Gabrieli, S., Reiss, A., Eberhardt, J. L., Gabrieli, J. D., et al. (2007). Differential development of high-level visual cortex correlates with category-specific recognition memory. *Nature Neuroscience*, *10*, 512–522.
- Gomez, J., Barnett, M. A., Natu, V., Mezer, A., Palomero-Gallagher, N., Weiner, K. S., et al. (2017). Microstructural proliferation in human cortex is coupled with the development of face processing. *Science*, *355*, 68–71.
- Goodale, M. A., & Milner, A. D. (1992). Separate visual pathways for perception and action. *Trends in Neurosciences*, *15*, 20–25.
- Grill-Spector, K., & Malach, R. (2004). The human visual cortex. *Annual Review of Neuroscience*, *27*, 649–677.
- James, K. H., & Kersey, A. J. (2017). Dorsal stream function in the young child: An fMRI investigation of visually guided action. *Developmental Science*, *21*, e12546.
- JASP Team. (2018). JASP (version 0.10.0) [computer software].
- Kersey, A. J., Clark, T. S., Lussier, C. A., Mahon, B. Z., & Cantlon, J. F. (2015). Development of tool representations in the dorsal and ventral visual object processing pathways. *Cerebral Cortex*, *26*, 3135–3145.
- Konen, C. S., & Kastner, S. (2008). Two hierarchically organized neural systems for object information in human visual cortex. *Nature Neuroscience*, *11*, 224–231.
- Kourtzi, Z., Erb, M., Grodd, W., & Bulthoff, H. H. (2003). Representation of the perceived 3-D object shape in the human lateral occipital complex. *Cerebral Cortex*, *13*, 911–920.
- Kovács, I., Kozma, P., Fehér, A., & Benedek, G. (1999). Late maturation of visual spatial integration in humans. *Proceedings of the National Academy of Sciences, U.S.A.*, *96*, 12204–12209.
- Kravitz, D. J., Saleem, K. S., Baker, C. I., Ungerleider, L. G., & Mishkin, M. (2013). The ventral visual pathway: an expanded neural framework for the processing of object quality. *Trends in Cognitive Sciences*, *17*, 26–49.
- Liu, T. T., Nestor, A., Vida, M. D., Pyles, J. A., Patterson, C., Yang, Y., et al. (2018). Successful reorganization of category-selective visual cortex following occipito-temporal lobectomy in childhood. *Cell Reports*, *24*, 1113.e6–1122.e6.
- Nishimura, M., Scherf, K. S., Zachariou, V., Tarr, M. J., & Behrmann, M. (2015). Size precedes view: developmental emergence of invariant object representations in lateral occipital complex. *Journal of Cognitive Neurosciences*, *27*, 474–491.
- Rosenthal, G., Tanzer, M., Simony, E., Hasson, U., Behrmann, M., & Avidan, G. (2017). Altered topology of neural circuits in congenital prosopagnosia. *eLife*, *6*, e25069.
- Saygin, Z. M., Osher, D. E., Norton, E. S., Youssoufian, D. A., Beach, S. D., Feather, J., et al. (2016). Connectivity precedes function in the development of the visual word form area. *Nature Neuroscience*, *19*, 1250–1255.
- Scherf, K. S., Behrmann, M., Humphreys, K., & Luna, B. (2007). Visual category-selectivity for faces, places and objects emerges along different developmental trajectories. *Developmental Science*, *10*, F15–F30.
- Scherf, K. S., Thomas, C., Doyle, J., & Behrmann, M. (2014). Emerging structure–function relations in the developing face processing system. *Cerebral Cortex*, *24*, 2964–2980.
- Simony, E., Honey, C. J., Chen, J., Lositsky, O., Yeshurun, Y., Wiesel, A., et al. (2016). Dynamic reconfiguration of the default mode network during narrative comprehension. *Nature Communications*, *7*, 12141.
- Ungerleider, L. G., & Mishkin, M. (1982). Two cortical visual systems. In D. J. Ingle, M. A. Goodale, & R. J. W. Mansfield (Eds.), *Analysis of visual behavior* (pp. 549–586). Cambridge, MA: MIT Press.
- Van Dromme, I. C., Premereur, E., Verhoef, B. E., Vanduffel, W., & Janssen, P. (2016). Posterior parietal cortex drives inferotemporal activations during three-dimensional object vision. *PLoS Biology*, *14*, e1002445.
- Vaziri-Pashkam, M., & Xu, Y. (2017). Goal-directed visual processing differentially impacts human ventral and dorsal visual representations. *Journal of Neuroscience*, *37*, 8767–8782.
- Wang, L., Mruczek, R. E., Arcaro, M. J., & Kastner, S. (2015). Probabilistic maps of visual topography in human cortex. *Cerebral Cortex*, *25*, 3911–3931.
- Zachariou, V., Nikas, C. V., Safiullah, Z. N., Gotts, S. J., & Ungerleider, L. G. (2017). Spatial mechanisms within the dorsal visual pathway contribute to the configural processing of faces. *Cerebral Cortex*, *27*, 4124–4138.